





Computer simulations as an effective way to distinguish supramolecular nanostructure in cyclic and phenyl alcohols

Joanna Grelska ^{1,*} Karolina Jurkiewicz ^{1,†} Andrzej Nowok ^{2,3} and Sebastian Pawlus ¹

¹*A. Chelkowski Institute of Physics, University of Silesia in Katowice, 75 Pułku Piechoty 1, 41–500 Chorzów, Poland*

²*Department of Experimental Physics, Wrocław University of Science and Technology,
Wybrzeże Stanisława Wyspiańskiego 27, 50–370 Wrocław, Poland*

³*Laboratoire National des Champs Magnétiques Intenses, UPR 3228, CNRS-UGA-UPS-INSA, Grenoble and Toulouse, France*



(Received 16 September 2022; accepted 2 July 2023; published 4 August 2023)

Molecular dynamics simulations supported by x-ray-diffraction experimental data were utilized to demonstrate how replacing the cyclic ring with the phenyl one in molecules of alcohols significantly differentiates their nanostructure by reducing the number of H-bonded clusters. Besides, molecules in the phenyl alcohols associate themselves in clusters via phenyl ring organization which likely is the result of $\text{OH} \cdots \pi$ and $\pi \cdots \pi$ interactions. Thus, at room temperature, the supramolecular structure of phenyl alcohols is more heterogeneous and governed by the formation of various clusters arising due to three types of interactions, while in cyclic alcohols, the H bonding controls the association of molecules. We believe that our methodology could be applied to better understand the fundamental process of association via H bonding and the competitive aggregation caused by phenyl rings.

DOI: [10.1103/PhysRevE.108.024603](https://doi.org/10.1103/PhysRevE.108.024603)

I. INTRODUCTION

The process of supramolecular aggregation on the nanoscale is the subject of extensive studies as it plays an important role in the properties and reactions of building blocks of living organisms such as proteins, polysaccharides, nucleotides in DNA chain, and other large biomolecules [1–7]. One of the most important driving forces for the supramolecular nanostructuring in biological systems are hydrogen bonds and $\pi \cdots \pi$ interactions of aromatic groups. These forces are considered while designing supramolecular solid-state architectures of self-assembled drug-delivery systems [8,9]. Therefore, knowledge of the organization of molecules in systems where hydrogen bonds and aromatic ring interactions cooperate is important for both fundamental science and technical applications. However, while the characterization of the structure of macromolecular complex systems is very demanding, more impact needs to be placed on simple model systems. Such a group is alcohols that create supramolecular clusters, in the size of a few nanometers, via hydrogen bonds formed by hydroxyl groups of molecules. Furthermore, the chemical structure of alcohols can be easily altered by attaching various functional groups. Especially, the hydrogen bond network can be suppressed when a steric hindrance, e.g., a carbon ring, is introduced in the neighborhood of the OH group [10,11]. However, up to now, there have been many misconceptions about how the association changes when the aromaticity of the functional groups is substituted.

Recent combined dielectric and photon-correlation spectroscopy studies conducted on alcohols with attached phenyl groups suggested that the formation of supramolecular clusters promoted by hydrogen bonds is not suppressed in those compounds compared to their aliphatic counterparts, but their architecture varies from chain- to ringlike shapes as the phenyl ring moves closer to the hydroxyl group [12]. In turn, a series of our recent papers based on dielectric, infrared, and diffraction investigations present a rather different view on the association of molecules in phenyl alcohols. Namely, we suggested that the phenyl ring may excite the organization of molecules via $\text{OH} \cdots \pi$ interactions and, as a consequence of this, cause a diverse packing of molecules on the short- and medium-range scale [13]. Moreover, we demonstrated that the population of hydrogen bonds is more abundant in cyclic (aliphatic) than phenyl (aromatic) compounds [14]. Furthermore, using computer simulations, we revealed that despite the lack of the diffraction prepeak, which was proved to be a fingerprint of the organization of hydroxyl groups into associates, phenyl alcohols tend to create small H-bonded clusters [15].

In this paper we use molecular dynamics simulations supported by x-ray diffraction to fill the gap in understanding the intermolecular structure of phenyl and cyclic alcohols in the liquid state at ambient conditions. The very good compliance between the experimental and molecular dynamics data prompted us to analyze the optimized structural models in detail using computational methods. We also confirmed our findings in experimental results of infrared and dielectric spectroscopy. Investigations on the compounds were performed at room temperature, as these conditions are the most suitable to track differences in the degree of association and intermolecular arrangements between aromatic

*joanna.grelska@us.edu.pl

†karolina.jurkiewicz@us.edu.pl

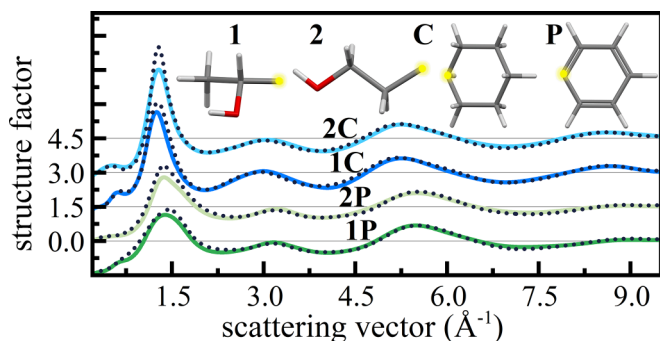


FIG. 1. Structure factors obtained from experiment (colored solid lines) and simulations (black dotted lines) for all investigated compounds. Models of their molecules are shown in upper part of graph as composed of two parts: alkyl chain (1 – or 2 –) and a hexagonal ring (C – cyclic, P – phenyl) with a connection linking both parts marked in yellow.

and nonaromatic H-bonded systems [10,11,13]. Namely, at room temperature, hydrogen bonds dominating in alcohols are weaker than at low temperatures and it is feasible to observe other interactions resulting from phenyl moiety.

II. METHODOLOGY

The investigated liquids are two isomers of phenyl alcohols: 1-phenylethanol (1P) and 2-phenylethanol (2P) with formula $C_8H_{10}O$, and their nonaromatic counterparts 1-cyclohexylethanol (1C) and 2-cyclohexylethanol (2C) with formula $C_8H_{16}O$, shown in the inset of Fig. 1. All compounds were purchased from Sigma-Aldrich. The difference between secondary (1) and primary (2) alcohols is in the positions of hydroxyl group relative to the carbon ring in the molecule. For simplicity, in the rest of the paper, the molecules with cyclic substituent will be called “cyclic” (C), while the aromatic ones will be alternatively called “phenyl” (P). The C and P alcohols in 1 and 2 configurations vary in the type of hexagonal carbon ring possessing very similar intramolecular architecture.

The experimental results were obtained at room temperature by wide-angle x-ray diffraction with Ag anode and normalized to the structure factor form (diffraction intensity per one atom). More details on the apparatus are contained in Ref. [15]. Molecular dynamics (MD) simulations were carried out using GROMACS package (version 2020) [16–18] at the NVT ensemble of 2000 molecules, at temperature 293.15 K. Topology files were created using the Antechamber module (AMBERTOOLS21) [19], and GAFF force field was used, which was developed for simulating organic compounds containing phenyl moieties [20]. Other parameters were analogous to those used in our previous paper [15]. Trajectories were collected after 2 ns of equilibration, from time of 2 ns. TRAVIS software [21–23] was used to calculate model-based structure factors, radial distribution functions, and combined functions of angular distribution versus radial distribution.

III. STRUCTURE PROPERTIES

The structure factors presented in Fig. 1 show very good compliance of the MD simulations with experimental re-

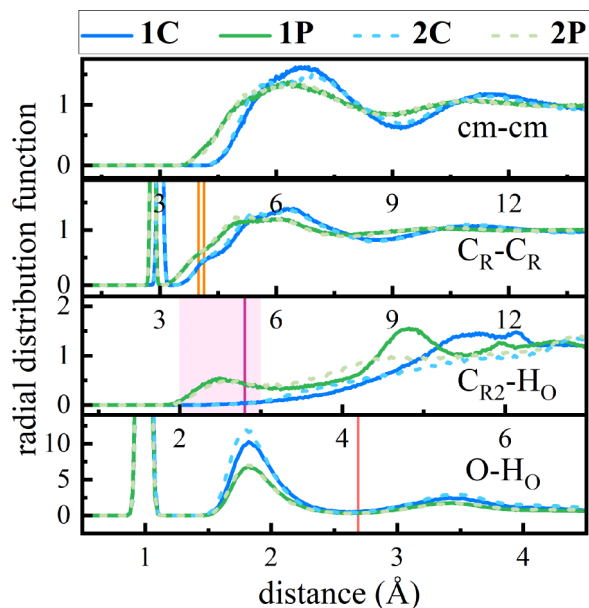


FIG. 2. Model-based radial distribution functions between centers of molecule masses, cm-cm, (top panel), as well as between first or fourth carbon atoms in rings, C_R-C_R ; fourth carbon atom in ring and hydrogen atom attached to oxygen, $C_{R2}-H_O$; oxygen and hydrogen attached to oxygen, $O-H_O$.

sults. Based on the data, one can see that the intermolecular structure of phenyl compounds 1P and 2P, manifested in low-scattering vectors up to $\sim 2.25 \text{ \AA}^{-1}$, differs significantly from that of cyclic counterparts 1C and 2C. The main diffraction peak of the aromatic systems is broader and has a clearly lower intensity in comparison to the aliphatic counterparts. That indicates a bigger disorder and heterogeneity of the nearest-neighbor intermolecular structure of phenyl alcohols. In turn, cyclic alcohols have clearly separated two values of the scattering vector in the range of intermolecular correlations: main-peak at $\sim 1.4 \text{ \AA}^{-1}$ and weaker prepeak at $\sim 0.7 \text{ \AA}^{-1}$. In real space, those translate to periodicities existing between nearest-neighbor molecules and groups of bonded molecules, respectively. What is interesting, the structure factor of phenyl compound 1P is also characterized by a weak prepeak at a similar position while for 2P the prepeak seems to be completely damped. On the molecular level, in 1P the distance between hydroxyl group and phenyl ring is 1 carbon atom while, for 2P, 2 carbon atoms separate the functional moieties. Therefore, one may expect a stronger steric hindrance on H bonding by the carbon ring in the case of 1P than 2P (and 1C than 2C). A detailed explanation of the prepeak feature is provided based on the simulated partial atom-atom structure factors in Supplemental Material [24].

Using the spatial organization of molecules optimized by the MD simulations, the radial distribution functions (rdfs) were calculated. Figure 2 shows the selected partial rdfs in the range of distances up to 4.5 \AA , where the intramolecular and short-contact intermolecular correlations give the main contribution. The intensity of the rdf peaks is proportional to the probability of finding two atoms (or groups of atoms) in

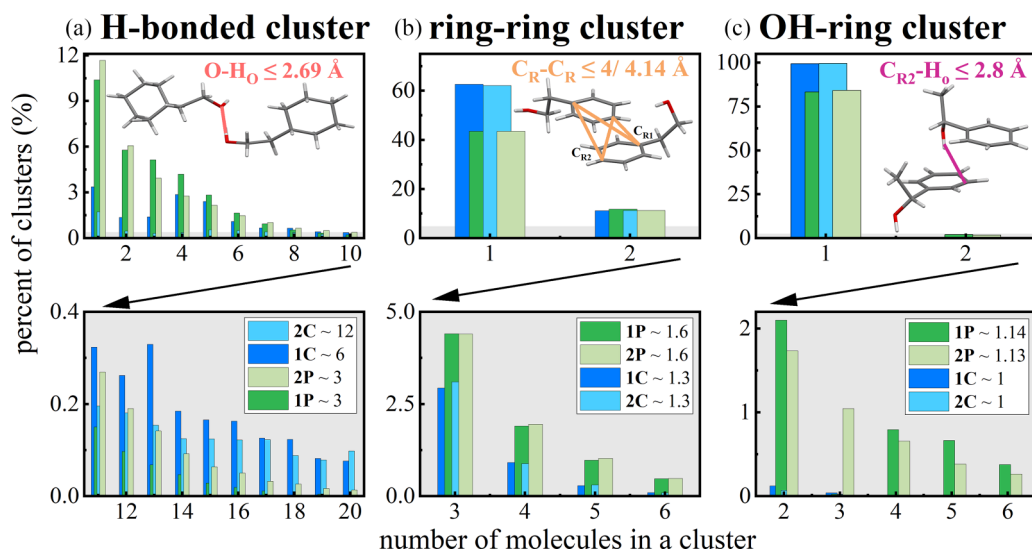


FIG. 3. Histograms of concentration of clusters obtained from optimized structural models as function of number of molecules associated in (a) H-bonded clusters, (b) ring clusters, and (c) OH-ring cluster. Average numbers of molecules in all types of clusters for all studied alcohols are depicted in legends on graphs. Distributions for higher values of molecules in a cluster are enclosed in separate graphs below. Criteria used for definition of all types of clusters are presented in insets.

the system at the given distance. A clear difference is visible again between the phenyl and cyclic alcohols. The former class is characterized by shorter distances between centers of molecular masses (cm-cm). This observation supports the fact that molecules in phenyl alcohols are more densely packed and have bigger molar density than their cyclic counterparts (see Supplemental Material [24] for density measurements). However, the differences in the packing of molecules between both types of alcohols can also originate from the distinct aggregation and stacking of phenyl and cyclic carbon rings.

In order to investigate this issue in more details, the C_{R-C_R} radial distribution function, which covers the correlations within and between the carbon rings, was calculated (Fig. 2). C_{R1} is the first carbon linking the ring with the tail of molecule and C_{R2} lies in the opposite position in the ring; see the scheme in Fig. 3. The C_{R-C_R} rdf follows a similar course above around 3 Å as the cm-cm function. The additional peak at the distance of around 2.8 Å, absent in the cm-cm function, originates from the intramolecular $C_{R1-C_{R2}}$ distances (ring diameter). It may be noticed that the diameter is slightly greater for more flexible cyclic molecules. The broad bump in the C_{R-C_R} function with maximum at around 6 Å, arising from the intermolecular correlations between carbon rings, is clearly shifted towards smaller distances for phenyl than cyclic alcohols. It raises the question about the arrangement of molecules at short distances, whether it is similar for phenyl and cyclic rings, or whether the effect of speculated $\pi\cdots\pi$ or $OH\cdots\pi$ interactions in the aromatic alcohols alters the structural organization.

The possible $OH\cdots\pi$ interactions would alter the arrangement of molecules in such a way that OH group of one molecule approaches the carbon ring of a neighboring molecule. Therefore, in order to detect such alignments we calculated the C_{R2-H_O} radial distribution function between the terminating carbon atom in the ring and hydrogen atom attached to oxygen. The average distance between the H_O

and C_{R2} atoms within the investigated molecules is bigger than 4 Å. Thus, the appearance of C_{R2-H_O} correlations at smaller distances would appear for an organization of C_{R2-H_O} atoms belonging to neighboring molecules. Indeed, a clear maximum at around 2.5 Å appears in the C_{R2-H_O} distribution function (marked in Fig. 2), but only for phenyl alcohols 1P and 2P. Thus, it confirms the spatial correlations of molecules where the $OH\cdots\pi$ interactions may occur. The distance is in the range of $OH\cdots\pi$ interaction reported in the literature (2.3–3 Å) [25,26].

Moreover, the $O-H_O$ radial distribution function, taking into account oxygen atoms and the hydrogen atoms attached to oxygens, is shown in the bottom panel of Fig. 2. It provides information about the spatial correlations of molecules connected by hydrogen bonds. The first peak of this function at a distance of around 1 Å results from the intramolecular $O-H_O$ connections. Further peaks can be assigned to the intermolecular distances. For all of the studied alcohols, the next maximum of the $O-H_O$ function appears around 1.8 Å and has a similar shape, suggesting that the pattern of H bonds and their strength does not differ significantly between the cyclic and phenyl alcohols. However, the intensity of this peak is clearly higher for cyclic compounds indicating a higher concentration of hydrogen bonds in those systems. The distance in which the intensity of $O-H_O$ peaks fades is around 2.69 Å for all samples. Therefore, that value can be taken as the maximum $O-H_O$ distance in the hydrogen-bonding pattern for all modeled systems.

All these results explain well some peculiarities observed in infrared spectroscopy studies on these compounds (see Fig. S2 in Supplemental Material [24]). In fact, Fourier transform infrared (FTIR) spectra of 1C and 2C contain a single broad OH stretching band which points to almost full association of OH groups [27]. Maximum of this band is shifted towards lower wave numbers for 2C, which (following previous reports) may indicate bigger H-bonded aggregates at

room temperature compared to the 1C isomer. Contrary to the cyclic alcohols, room-temperature FTIR spectra of the phenyl analogs, beside OH stretching band, contain less-intense band which, following previous reports [8,9,11], we attribute as a stretching mode of the OH groups involved in OH- π interactions. Hence, its occurrence in the case of phenyl alcohols indicates that they associate to some extent by OH- π forces and therefore their degree of intermolecular association via hydrogen bonds at room temperature is lower than for cyclic alcohols. Additionally, higher full width at half maximum of the OH stretching band of phenyl alcohols confirms more heterogeneous distribution of the H-bonded agglomerates.

IV. CLUSTER ANALYSIS

The presented structural correlations between atoms belonging to different molecules prove the supramolecular organization of the studied alcohols. However, the clustering pattern is significantly different between molecules with cyclic and phenyl rings. In order to deepen the analysis of the obtained models, the number of molecules in various supramolecular clusters was calculated using the `gmx_cluster` program in GROMACS package. Three types of clusters were considered.

The first type of clustering is prompted by the H bonding. The criterion for a molecule to be associated in the cluster linked by H bonds was taken as the distance between O and H_O atoms of neighboring molecules smaller than 2.69 Å, based on the cutoff of the O-H_O radial distribution function (ticked in Fig. 2). That distance also covers the usual H-bonding criteria, which are O-OH angle $\leq 30^\circ$ and O-O distance ≤ 3.5 Å, based on the triangle relation. As can be seen from the cluster distributions in Fig. 3(a), for 2P and 1P the number of molecules unassociated in H-bonded clusters (single molecules) is much higher ($\sim 10\%$) than for cyclic compounds ($\sim 2\%$). Thus, the proposed models exhibit a destructive effect of carbon-ring aromaticity on the H-bond connections. As can be retrieved from the average number of molecules in such clusters, the alcohol that creates the largest H-bonded clusters is cyclic 2C (12 molecules), then 1C (6 molecules), and the smaller clusters, composed of 3 molecules on average, form 2P and 1P. The determined average cluster size is strongly dominated by large clusters, occurring especially in the cyclic alcohols. Thus, the most probable cluster size, which is 5–6 and 4 molecules for 2C and 1C, respectively, provides a more realistic picture of these structures. Moreover, the effect of the steric hindrance induced by the location of the OH group in the short distance relative to the carbon ring is significant in the case of cyclic alcohols: 1C has more unassociated molecules and creates smaller clusters of H-bonded molecules, on average, than 2C. In turn, for phenyl alcohols, the position of the OH group has much smaller impact on the average size of H-bonded associates.

The second type of clusters analyzed in the optimized models concerned the organization of carbon rings—we will call them “ring clusters.” The above-presented cm-cm and C_R-C_R radial distribution functions demonstrated significant differences in the structuring of rings between the cyclic and phenyl compounds. As a criterion for the ring cluster, the maximum distance between C_{R1} or C_{R2} of all atoms in

molecules was taken as 4 Å for phenyl compounds and 4.14 Å for cyclic ones (ticked in Fig. 2). These values were chosen to be higher than ring diameter and at the lower limit of cm-cm distance. The value for cyclic alcohols was increased, taking into account the density proportion (~ 0.92 g/cm³ for cyclic and ~ 1 g/cm³ for phenyl compounds). It is worth noting that similar $\pi\cdots\pi$ interaction distance, around 3.8 Å, was found in the face-to-face alignment of phenyl-ring centroids [28]. The histograms of the ring clusters are shown in Fig. 3(b). Accordingly, 40% of all cyclic and 60% of all phenyl molecules are associated in ring clusters. Dimers are the most abundant type of ring associates—involving above 10% of phenyl molecules. In turn, the ring dimers in cyclic alcohols constitute below 10% of all molecules and the concentration of bigger ring clusters is negligible. The average number of molecules in the ring cluster (1.6 for phenyl and 1.3 for cyclic alcohols) supports the idea that phenyl alcohols exhibit a stronger tendency toward ring organization than cyclic alcohols, caused by their ability to form $\pi\cdots\pi$ interactions.

The third type of cluster is induced by OH $\cdots\pi$ arrangement and called “OH-ring cluster.” In order to calculate the distribution of this cluster we chose carbon atom C_{R2} and hydrogen next to oxygen H_O, the same as presented in the rdf function, with the limit value of 2.8 Å (ticked in Fig. 2). The obtained results in Fig. 3(c) show that this type of cluster does not occur in cyclic compounds, while in phenyl ones they are significant (constitute around 20%). A little bit higher probability of such OH-ring cluster exists for 1P than for 2P, which has more favorable location of OH group for this kind of cluster arrangement.

In order to illustrate the spatial organization of molecules in the investigated models, the selected plane cuts of the simulation boxes are presented in Fig. 4. For a clear presentation of the discussed H-bonded and ring clusters, molecular skeletons without H atoms are shown in the left column while in the right column neat OH groups were extracted. For 2C alcohol, one can see that OH groups link into long chains the size of a few nanometers. There are no visible free molecules. The structure of 1C consists of shorter OH chains and other small clusters. From the histogram [Fig. 3(a)] one can see that 1C has a tendency to group into four molecules, which is confirmed in the picture of the organization of molecules and H bonds in Fig. 4. In the case of phenyl compounds 1P and 2P, there are only short H-bonded chains of few molecules, and many molecules are not linked with each other.

A closer look at the models allows us to notice that the aggregation of carbon rings is a characteristic feature of phenyl compounds. There is a great diversity of the arrangements adopted by molecules in such ring-ring clusters: *T* type, parallel, offset parallel, and perpendicular shaped, which are marked in light orange in Fig. 4. Similar configurations were reported for benzene—the archetypal aromatic system exhibiting $\pi\cdots\pi$ interactions [29]. Besides the molecular layouts supporting the existence of $\pi\cdots\pi$ interactions in phenyl alcohols, the models also exhibit the arrangement of molecules where OH $\cdots\pi$ interaction may occur (see clusters marked in light pink in Fig. 4). On the other hand, such arrangements in the models of cyclic alcohols are rare and incidental.

These outcomes explain well the differences in dielectric response of alcohols with cyclic and phenyl rings. Namely,

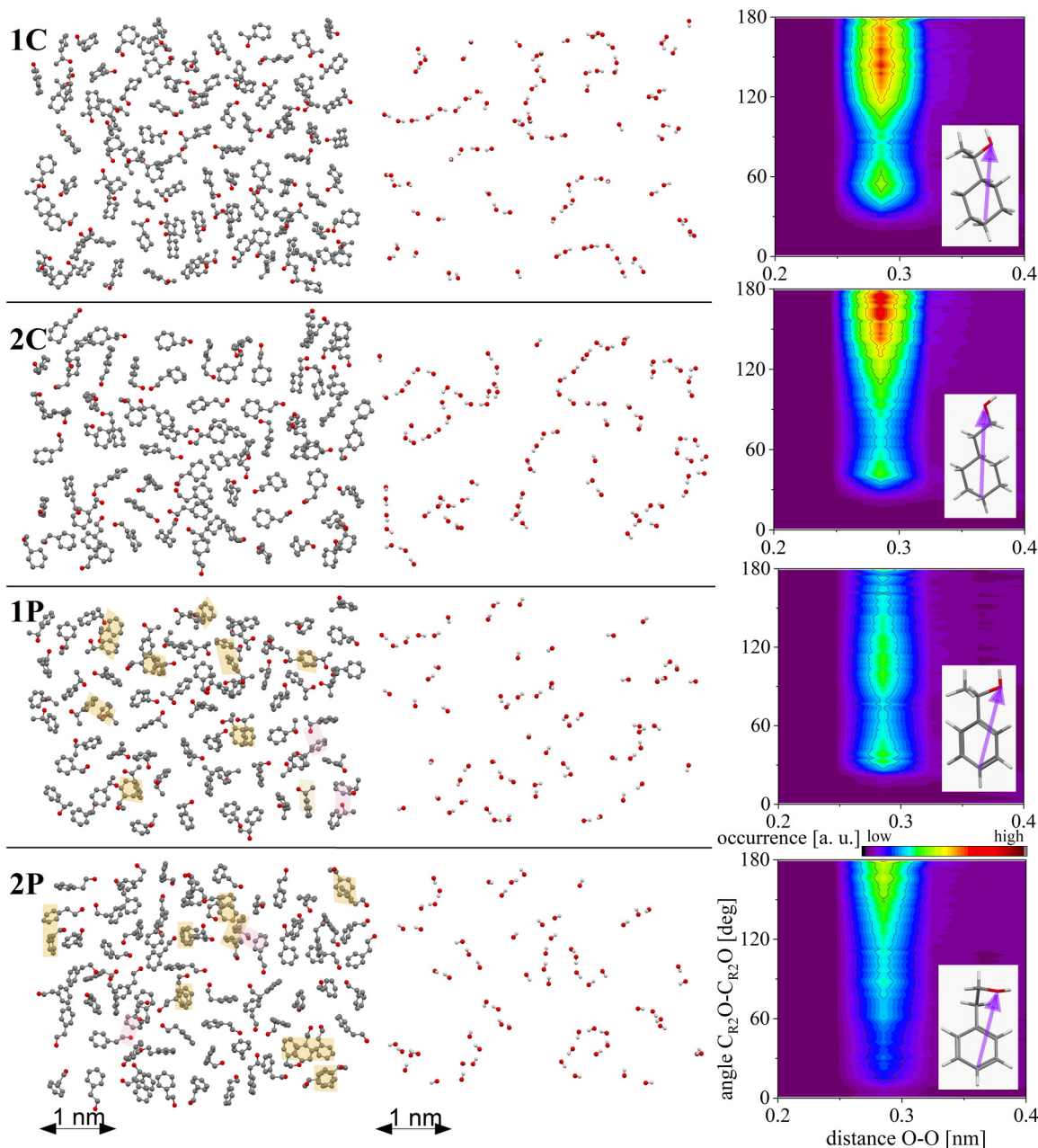


FIG. 4. Two-dimensional planes cut from the optimized structural models of cyclic and phenyl alcohols. (Left) Skeletons of molecules without hydrogen atoms are presented for clarity. In next column, only OH groups extracted from molecules are displayed. Centroids of molecular fragments fitting in planes are presented in each case. Therefore, these two representations differ in number of visible O and OH groups. For 1P and 2P possible $\pi \cdots \pi$ and $\text{OH} \cdots \pi$ related arrangements are marked in light orange and pink, respectively. (Right) Combined functions of angular distribution $\text{C}_{\text{R}_2\text{O}}\text{-C}_{\text{R}_2\text{O}}$ vs O-O radial distribution. Purple arrows mark molecules' chosen vectors in insets.

a characteristic feature of MD of alcohols is the Debye process, which reflects the mobility of the supramolecular nanostructures with a nonzero resultant dipole moment [27]. It was observed that a well-separated Debye peak of a high amplitude characterizes the dielectric spectra of alcohols with cyclohexyl ring (including 1C and 2C) [13,14]. In turn, dielectric spectra of aromatic alcohols such as 1P and 2P contain broadened Debye peaks of relatively low amplitude, additionally characterized by a small separation from the structural relaxation [10,13]. Our

studies show that these features are strictly connected with the small size of H-bonded clusters, as well as more heterogeneous supramolecular nanostructure due to $\pi \cdots \pi$ and $\text{OH} \cdots \pi$ arrangements.

Finally, we investigated the mutual alignment of molecules in their theoretical models derived from MD simulations. The intermolecular angular distributions of the selected vectors with reference to the intermolecular oxygen-oxygen distance were derived using TRAVIS software (Fig. 4). Vectors of molecules start from the terminating carbon atom C_{R_2} and

end in the most electronegative oxygen atom O (see inset of Fig. 4 for visualization of the vectors). From graphs presented in Fig. 4 one can clearly notice the highest intensity in distributions for cyclic compounds. That is in line with the fact that these compounds tend to associate strongly through hydrogen-bond interaction and therefore give the highest contribution to O-O rdf function. The difference is, however, visible in the angular distribution of intensity. The nearest molecules in 2C tend to align antiparallel, which confirms the chainlike type of H-bonded clusters. In 1C the dominating vectors' angle covers the range of 100° – 180° that is most likely the result of the formation of more branched systems of H bonds in clusters. The phenyl equivalents mimic the angular distributions of cyclic compounds. Most likely to create branchedlike cluster formations is 1P; 2P molecules with the highest intensity of 180° tend to stack in the antiparallel manner.

The above statements are in agreement with the behavior of Kirkwood-Fröhlich correlation factor g_k , which is the parameter providing information on cross correlation of dipole moments between adjacent molecules (see our results in Fig. S3 in Supplemental Material [24]). Value of $g_k > 1$ indicates parallel arrangement of dipole moments (chainlike structure) while $g_k < 1$ suggests negative cross correlation (circular structure). As presented in Fig. S3, there are clear differences in g_k between the studied alcohols at room temperature. Under these conditions, the nonaromatic 2C distinguishes itself by the highest value of g_k (which exceeds 2), suggesting the preferred chainlike organization of molecules within the aggregates. Alcohols 1C and 2P are characterized by lower value of g_k , indicating less occurrence of linear structures and more heterogeneous or branched ones. In turn, the sterically hindered aromatic 1P alcohol is characterized by the lowest g_k

value, close to 1, which suggests a heterogeneous alignment of adjacent dipole moment vectors.

V. SUMMARY

To sum up, we probed the structure of two isomers of simple cyclic alcohols and their phenyl counterparts to describe in details their supramolecular nanostructure. It was demonstrated that cyclic compounds tend to associate into long H-bonded chains. In phenyl alcohols, the association by H bonds is damped compared to cyclic compounds while additional phenyl ring aggregation, related to $\pi\cdots\pi$ and $\text{OH}\cdots\pi$ interactions, arises. The model of the structure of phenyl compounds consists mostly of dimeric and trimeric H-bonded clusters and dimers aggregated by the aromatic rings or by the ring and OH group. Our results explain at the molecular level some previous assumptions derived by infrared studies (formation of $\text{OH}\cdots\pi$ interactions) and dielectric spectroscopy (occurrence of the Debye process, the behavior of the Kirkwood-Fröhlich factor) for phenyl and cyclic compounds. We believe the provided pictures of the structure of such model compounds will be vitally useful to better understand the structural properties of complex systems where multiple weak interactions, such as hydrogen and π - π bonds, participate in the formation of the supramolecular nanostructure.

ACKNOWLEDGMENTS

J.G., K.J., and S.P. are thankful for the financial support from the National Science Centre, Poland within the OPUS Project No. UMO-2019/35/B/ST3/02670. The authors thank Prof. A. Burian for guidance in the treatment of experimental diffraction data.

-
- [1] V. Basavalingappa *et al.*, Mechanically rigid supramolecular assemblies formed from an Fmoc-Guanine conjugated peptide nucleic acid, *Nat. Commun.* **10**, 5256 (2019).
 - [2] A. Arinstein, M. Burman, O. Gendelman, and E. Zussman, Effect of supramolecular structure on polymer nanofibre elasticity, *Nat. Nanotechnol.* **2**, 59 (2007).
 - [3] B. J. G. E. Pieters, M. B. van Eldijk, R. J. M. Nolte, and J. Mecnović, Natural supramolecular protein assemblies, *Chem. Soc. Rev.* **45**, 24 (2016).
 - [4] M. Diener, J. Adamcik, A. Sánchez-Ferrer, F. Jaedig, L. Schefer, and R. Mezzenga, Primary, secondary, tertiary and quaternary structure levels in linear polysaccharides: From random coil, to single helix to supramolecular assembly, *Biomacromolecules* **20**, 1731 (2019).
 - [5] S. L. Higashi, N. Rozi, S. A. Hanifah, and M. Ikeda, Supramolecular architectures of nucleic acid/peptide hybrids, *Int. J. Mol. Sci.* **21**, 9458 (2020).
 - [6] S. Cichosz and A. Masek, IR study on cellulose with the varied moisture contents: Insight into the supramolecular structure, *Materials* **13**, 4573 (2020).
 - [7] J. Paturej, K. Koperwas, M. Tarnacka, K. Jurkiewicz, P. Maksym, J. Grelska, M. Paluch, and K. Kamiński, Supramolecular structures of self-assembled oligomers under confinement, *Soft Matter* **18**, 4930 (2022).
 - [8] H. W. Roesky and M. Andruh, The Interplay of coordinative, hydrogen bonding and π - π stacking interactions in sustaining supramolecular solid-state architectures, *Coord. Chem. Rev.* **236**, 91 (2003).
 - [9] W.-R. Zhuang, Y. Wang, P.-F. Cui, L. Xing, J. Lee, D. Kim, H.-L. Jiang, and Y.-K. Oh, Applications of π - π stacking interactions in the design of drug-delivery systems, *J. Controlled Release* **294**, 311 (2019).
 - [10] A. Nowok, K. Jurkiewicz, M. Dulski, H. Hellwig, J. G. Małecki, K. Grzybowska, J. Grelska, and S. Pawlus, Influence of molecular geometry on the formation, architecture and dynamics of H-bonded supramolecular associates in 1-phenyl alcohols, *J. Mol. Liq.* **326**, 115349 (2021).
 - [11] A. Nowok, M. Dulski, K. Jurkiewicz, J. Grelska, A. Z. Szeremeta, K. Grzybowska, and S. Pawlus, Molecular stiffness and aromatic ring position – crucial structural factors in the self-assembly processes of phenyl alcohols, *J. Mol. Liq.* **335**, 116426 (2021).
 - [12] T. Böhmer, J. P. Gabriel, T. Richter, F. Pabst, and T. Blochowicz, Influence of molecular architecture on the dynamics of H-

- bonded supramolecular structures in phenyl-propanols, *J. Phys. Chem. B* **123**, 10959 (2019).
- [13] A. Nowok, M. Dulski, J. Grelska, A. Z. Szeremeta, K. Jurkiewicz, K. Grzybowska, M. Musiał, and S. Pawlus, Phenyl ring: A steric hindrance or a source of different hydrogen bonding patterns in self-organizing systems? *J. Phys. Chem. Lett.* **12**, 2142 (2021).
- [14] N. Soszka *et al.*, Aromaticity effect on supramolecular aggregation. aromatic vs. cyclic monohydroxy alcohols, *Spectrochim. Acta, Part A* **276**, 121235 (2022).
- [15] J. Grelska, K. Jurkiewicz, A. Burian, and S. Pawlus, Supramolecular structure of phenyl derivatives of butanol isomers, *J. Phys. Chem. B* **126**, 3563 (2022).
- [16] M. J. Abraham, T. Murtola, R. Schulz, S. Páll, J. C. Smith, B. Hess, and E. Lindahl, GROMACS: High performance molecular simulations through multi-level parallelism from laptops to supercomputers, *SoftwareX* **1–2**, 19 (2015).
- [17] S. Páll, M. J. Abraham, C. Kutzner, B. Hess, and E. Lindahl, Tackling exascale software challenges in molecular dynamics simulations with GROMACS, in *Solving Software Challenges for Exascale*, edited by S. Markidis and E. Laure (Springer International Publishing, Cham, 2015), Vol. 8759, pp. 3–27.
- [18] S. Pronk *et al.*, GROMACS 4.5: A high-throughput and highly parallel open source molecular simulation toolkit, *Bioinformatics* **29**, 845 (2013).
- [19] D. A. Case, H. M. Aktulga, K. Belfon, I. Y. Ben-Shalom, S. R. Brozell, D. S. Cerutti, T. E. Cheatham III, G. A. Cisneros, V. W. D. Cruzeiro, T. A. Darden, R. E. Duke, G. Giambasu, M. K. Gilson, H. Gohlke, A. W. Goetz, R. Harris, S. Izadi, S. A. Izmailov, C. Jin, K. Kasavajhala *et al.*, *Amber 2021, AmberTools21* (University of California, San Francisco, 2021).
- [20] J. Wang, R. M. Wolf, J. W. Caldwell, P. A. Kollman, and D. A. Case, Development and testing of a general amber force field, *J. Comput. Chem.* **25**, 1157 (2004).
- [21] M. Brehm and B. Kirchner, TRAVIS - A free analyzer and visualizer for Monte Carlo and molecular dynamics trajectories, *J. Chem. Inf. Model.* **51**, 2007 (2011).
- [22] O. Hollóczki, M. Macchiagodena, H. Weber, M. Thomas, M. Brehm, A. Stark, O. Russina, A. Triolo, and B. Kirchner, Triphasic ionic-liquid mixtures: Fluorinated and non-fluorinated aprotic ionic-liquid mixtures, *ChemPhysChem* **16**, 3325 (2015).
- [23] M. Brehm, M. Thomas, S. Gehrke, and B. Kirchner, TRAVIS—A free analyzer for trajectories from molecular simulation, *J. Chem. Phys.* **152**, 164105 (2020).
- [24] See Supplemental Material at <http://link.aps.org/supplemental/10.1103/PhysRevE.108.024603> for simulated partial atom-atom structure factors; density measurements; infrared spectroscopy measurements; and Kirkwood factors calculated based on dielectric spectroscopy measurements. Supplemental Material also contains Refs. [10,11,15].
- [25] K. Shin-ya, H. Sugeta, S. Shin, Y. Hamada, Y. Katsumoto, and K. Ohno, Absolute configuration and conformation analysis of 1-phenylethanol by matrix-isolation infrared and vibrational circular dichroism spectroscopy combined with density functional theory calculation, *J. Phys. Chem. A* **111**, 8598 (2007).
- [26] Q.-S. Du, Q.-Y. Wang, L.-Q. Du, D. Chen, and R.-B. Huang, Theoretical study on the polar hydrogen- π ($H\pi-\pi$) interactions between protein side chains, *Chem. Cent. J.* **7**, 92 (2013).
- [27] R. Böhmer, C. Gainaru, and R. Richert, Structure and dynamics of monohydroxy alcohols—milestones towards their microscopic understanding, 100 years after Debye, *Phys. Rep.* **545**, 125 (2014).
- [28] C. Janiak, A critical account on $\pi-\pi$ stacking in metal complexes with aromatic nitrogen-containing ligands, *J. Chem. Soc. Dalton Trans.* **21**, 3885 (2000).
- [29] T. F. Headen, Temperature dependent structural changes in liquid benzene studied using neutron diffraction, *Mol. Phys.* **117**, 3329 (2019).